Draft version September 16, 2020
Preprint typeset using LaTeX style emulateapj v. 12/16/11

THE CLUSTERS HIDING IN PLAIN SIGHT (*CHiPS*) SURVEY: CHIPS1911+4455 (PHOENIX MEETS EL GORDO)

Taweewat Somboonpanyakul[1], Michael McDonald[1], Matthew Bayliss, Mark Voit, Megan Donahue, Haakon Dahle, Emil Rivera-Thorsen, Brian Stalder[3], and Antony Stark[4]

Draft version September 16, 2020

ABSTRACT

We present high resolution optical images from *Hubble*, X-ray images from *Chandra*, and optical spectra from the Nordic Optical Telescope for the recently discovered galaxy cluster, CHIPS1911+4455 at $z = 0.485$. CHIPS1911+4455 is one of the two new clusters discovered in the Clusters Hiding in Plain Sight (*CHiPS*) survey with a goal to search for galaxy clusters with extreme central sources that were misidentified as isolated X-ray point sources in the ROSAT All-Sky Survey. With new *Chandra* X-ray observations, we determine the core density (∼10 kpc) to be 0.0884 cm^{-3} and the core entropy to be 17^{+2}_{-9} keVcm^2, suggesting a strong cool core, which are almost exclusively found at the centers of relaxed clusters. However, the large-scale morphology of CHIPS1911+4455 is highly asymmetric, pointing to a more disturbed cluster. Furthermore, the *Hubble* images reveal a massive, filamentary starburst near the brightest cluster galaxy (BCG). We measure the star formation rate for the BCG to be 120–140 $M_\odot\,yr^{-1}$, which is one of the highest rates measured in a central cluster galaxy to date. One possible scenario for CHIPS1911+4455 is that a part of the cool core was displaced from a major merger with other clusters, and that gas then cooled as it fell back to the core. This unique system is an excellent case study for high-redshift clusters which tend to have similar properties, i.e., having large star formation during a merger. Further studies of such systems will drastically improve our understanding of the relation between a merger and star formation in a cluster core and how this mechanism fits in the bigger picture of active galactic nuclei (AGN) feedback.

Subject headings: galaxies: clusters: general — galaxies: clusters: intracluster medium — X-rays: galaxies: clusters

1. INTRODUCTION

Clusters of galaxies are the largest gravitationally bound systems in the universe. Early X-ray observations of intracluster medium (ICM) in the center of clusters reveal that the gas was so dense that its cooling time was much shorter than the Hubble time, which led to the development of the cooling flow model (see review by Fabian (1994)). In this model, large amount of the hot gas in dense cores should have hydrostatically cooled and fueled 100–1000 $M_\odot\,yr^{-1}$ starbursts in the central brightest cluster galaxies (BCGs). However, many studies have shown that the gas has not cooled at the rate predicted by the model. In fact, most clusters only cool at ∼1% efficiency (McDonald et al. 2018). A promising mechanism proposed for preventing cooling of the ICM is AGN heating by jets and bubble-induced weak shocks (Fabian 2012; McNamara & Nulsen 2012). Several evidence supporting the theory includes the presence of radio galaxies at the center of clusters (Sun 2009) and the comparability between the mechanical energy released by AGN driven bubbles and the energy needed to quench cooling (e.g. Rafferty et al. 2008; Bîrzan et al. 2008; Hlavacek-Larrondo et al. 2015).

Galaxy clusters with high cooling efficiency of a few percent are often called "cool-core" (CC) clusters because of their highly-dense cores in the center of clusters (Molendi & Pizzolato 2001). The other class of clusters which do not host any obvious central core are commonly referred to as "non cool-core" clusters. Hudson et al. (2010) found that the best way to segregate the two is to consider their central cooling time (t_{cool}). Specifically, clusters with $t_{cool} < 7.7$ Gyr are considered hosting CCs while clusters with $t_{cool} < 1.0$ Gyr are believed to have strong CCs. A number of observational studies have found that cool cores are mostly found in relaxed clusters while non-cool cores are resided in disturbed clusters. As a matter of fact, clusters with the highest rate of cooling (∼10% instead of 1%) and hosting strong CCs, such as Abell 1835 (McNamara et al. 2006), H1821+643 (Russell et al. 2010), and the Phoenix cluster (McDonald et al. 2012), are among the most relaxed clusters we known. On the other hand, one of the most disturbed clusters, El Gordo (Menanteau et al. 2012), shows no sign of cooling or star formation near the center of the cluster. One of the main mechanism explaining disturbed clusters is major mergers which have a potential to destroy cool cores (Burns et al. 2008; Poole et al. 2008) through shock-heating (Burns et al. 1997) and mixing the ICM (Gómez et al. 2002). This is also consistent with Crawford et al. (1999); Donahue et al. (2010)'s works which found that star formation in BCGs is maximum in the most relaxed cool core clusters.

Therefore, the recent discovery of CHIPS1911+4455 is completely unexpected since it not only harbors a very blue galaxy in the center, which is a signature for a strong cooling system similar to the Phoenix cluster, but also

[1] Kavli Institute for Astrophysics and Space Research, Massachusetts Institute of Technology, 77 Massachusetts Avenue, Cambridge, MA 02139
[3] LSST, 950 N. Cherry Ave, Tucson, AZ 85719, USA
[4] Harvard-Smithsonian Center for Astrophysics, 60 Garden St., Cambridge MA 02138, USA

shows a highly-disturbed morphology on both large (∼50 kpc) and small (∼20 kpc) scales (Somboonpanyakul et al. in prep.). There is basically no known nearby object that has properties similar to CHIPS1911+4455. Nevertheless, McDonald et al. (2016) reported that high-redshift BCGs ($z > 1$) with large star formation rate (SFR) tend to be in merging clusters, unlike low-redshift BCGs with high SFR which usually are in relaxed systems. This implies that CHIPS1911+4455 could potentially be a prime example for studying high-redshift clusters. To fully understand how a disturbed system can sustain both a strong cool core and a blue galaxy in the center, we obtain new observations in the core of CHIPS1911+4455. The data presented in this paper includes high-resolution optical images from the *Hubble* Space Telescope (HST), X-ray images from *Chandra*, and optical spectra from Nordic Optical Telescope (NOT).

The remainder of this paper is structured as follows. We highlight the "Cluster Hiding in Plain Sight" (CHiPS) survey in Section 2. A complete summary of the survey can be found in previous publications (Somboonpanyakul et al. 2018). In Section 3, we present details for the data reduction/analysis for *Chandra*, *Hubble*, and the NOT spectrum. The results from these data are presented in Section 4. We discuss the implication of this discovery in Section 5 before concluding our results in Section 6. We assume $H_0 = 70\,\mathrm{km\,s^{-1}Mpc^{-1}}$, $\Omega_m = 0.3$, and $\Omega_\Lambda = 0.7$. All errors are $1\,\sigma$ unless noted otherwise.

2. THE CHIPS SURVEY

CHIPS1911+4455, at RA=19h11m01s and Dec=44d55m20s, was first discovered, and later confirmed with the *Chandra* X-ray images, as a result of the Clusters Hiding in Plain Sight (*CHiPS*) survey, which aims to find galaxy clusters hosting extreme central galaxies such that they were misclassified as point sources in the ROSAT All-Sky Survey (Somboonpanyakul et al. 2018, 2020 in prep.). We achieved this by searching for an overdensity of red galaxies surrounding these bright X-ray-, mid-IR-, and radio-bright sources, using both archival all-sky survey data (e.g., Sloan Digital Sky Survey (SDSS; Gunn et al. 2006; Abolfathi et al. 2018) and PAN-STARR (Chambers et al. 2016)) and newly obtained data from the 6.5m Magellan telescope with the Parallel Imager for Southern Cosmological Observations (PISCO; Stalder et al. 2014).

3. OBSERVATIONS

In this section, we summarize the acquisition and reduction of data obtained and used in this work, including the X-ray data from the *Chandra* X-ray telescope, the high-resolution images from the *Hubble* Space Telescope and the optical spectra from the Nordic Optical Telescope (NOT). The *Hubble* images provide an order of magnitude improvement in depth and angular resolution, compared to archival Pan-STARRS images, used during our initial discovery period of the *CHiPS* survey. These images allow us to look for extended cooling filaments and/or additional galaxies in a case of a major merger event. Whereas, the optical spectra from the NOT telescope contain information about the properties of the BCG and precise redshift measurement for the cluster. These data, as well as the previously-obtained *Chandra* image, will allow us to constrain properties of the cluster and study characteristics of the extreme central galaxy.

3.1. *X-ray: Chandra*

CHIPS1911+4455 (OBS ID: 21544) was observed in 2019 with *Chandra* ACIS-I for a total of 30.5 ks. The data were analyzed with `CIAO` version 4.11 and `CALDB` version 4.8.5, provided by the Chandra X-ray Center (CXC). It was recalibrated with VFAINT mode for improved background screening. In order to look for small-scale structures near the center of the cluster, images were smoothed adaptively, using `CHSMOOTH`[4] which smooths images on variable scales to achieve a uniform signal-to-noise ratio over the full image, as shown in the left panel of Fig. 1.

The temperature profile was extracted from spectra with coarse annuli so that the number of counts per annulus was around 800, which is enough to get well-constrained temperature measurements (ΔkT/kT ∼20%). All the spectra were fit simultaneously with the `APEC` models for both the cluster and the Milky Way, Galactic absorption, and thermal bremsstrahlung from unresolved background with a temperature of 40 keV, similar to what was done in (McDonald et al. 2014). The *WSTAT* statistic was used.

The radial gas density profile was created by obtaining the numbers of counts at 0.7-2.0 keV in concentric annuli and dividing them by the annulus area to get the surface brightness profile. Then, the normalization for each annulus was calculated individually to convert the profile to the emission-measure profile ($\mathrm{EM}(r) = \int n_p n_e dl$), based on the temperature at each bin according to the temperature profile. The conversion factors came from estimating the normalization for the collisionally-ionized plasma `APEC` model whose number of counts is the same as the extracted number of counts for each bin.

3.2. *Optical: Hubble*

The center of CHIPS1911+4455 was observed with the *Hubble* Space Telescope (HST) during Cycle 27 Mid-Cycle. The data include broad band F550M (1 orbit) and F110W (1 orbit), using the Advance Camera for Surveys(ACS)/Wide Field Camera (WFC). The F550M filter contains both the blue continuum and the bright [OII] doublets at the redshift of the cluster, representing young star-forming regions. Whereas, F110W covers the red continuum which depicts both the elliptical BCG and its red cluster members.

3.3. *Optical Spectra: Nordic Telescope*

The two optical spectra of the BCG of CHIPS1911+4455 were obtained with the Alhambra Faint Object Spectrograph and Camera (ALFOSC) at the 2.56m Nordic Optical Telescope (NOT). One of the spectra was obtained from Grism#4 (R = 360) with 1.3" slit for 1500-second exposure. The other spectrum was a stack of two 1100-second spectra from Grism#5 (R = 415) with 1.3" slit at 90° from the first spectrum. Wavelengths for the two spectra were calibrated with HeNe and ThAr arc lamps, respectively. Masks were applied to remove cosmic-rays before the 1D spectra

[4] https://cxc.harvard.edu/ciao/ahelp/csmooth.html

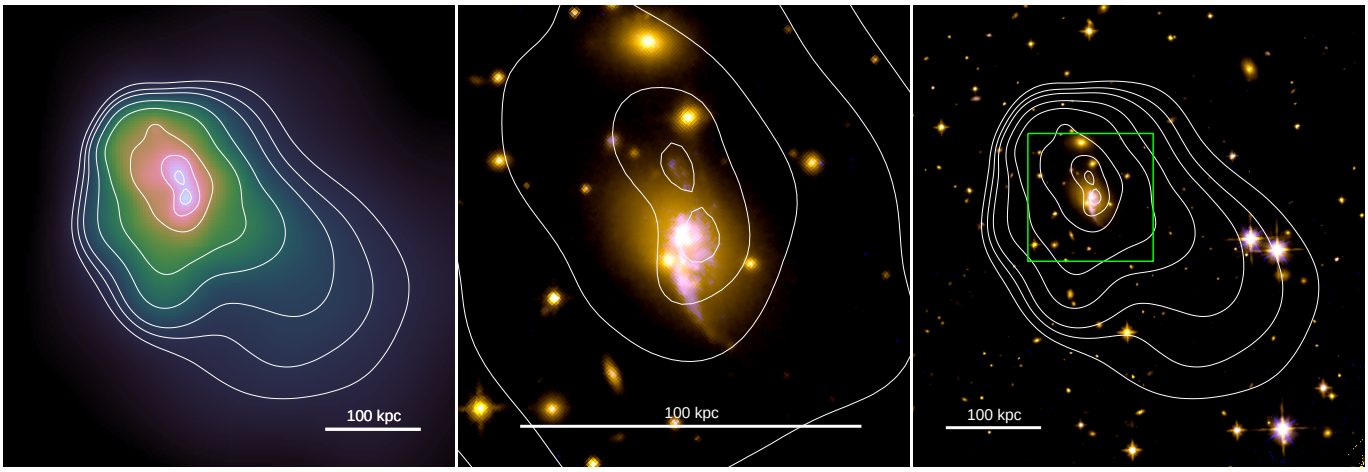

FIG. 1.— Left: *Chandra* 0.5-7.0 keV image of CHIPS1911+4455, highlighting the asymmetric morphology on both small and large scales with either one or two distinct cool cores. Middle: The *Hubble* images of the central galaxy, showing the star-forming filaments, extending on scales of $\sim$ 30 kpc. Right: The *Hubble* images with an overlay of the X-ray contour on top. These images show the direction of the extended hot gas in relation to the direction of the blue complex filaments, suggesting that the two might be connecting together.

were extracted from the 2D spectral images. The 1D spectra were then normalized from off-source regions surrounding the 1D extraction region.

4. RESULTS

4.1. *CHIPS1911+4455: A Strong Cool Core*

The left panel of Fig. 3 shows the surface brightness profile of the cluster out to $\sim$1000 kpc. The inner core density at 10 kpc is $0.0884\,\mathrm{cm}^{-3}$, which is among the highest measured to date (McDonald et al. 2017). Meanwhile, the temperature profile in the right panel of Fig. 3 also exhibits a temperature gradient from 4 keV at $\sim$10 kpc to a maximum of $\sim$8 keV at $\sim$300 kpc. We do not have enough data to constrain the temperature profile out to a larger radii.

The entropy of the ICM can be calculated using $K(r) = kT(r) \times n_e(r)^{-2/3}$, where $kT(r)$ is the temperature profile and $n_e(r)$ is the electron density profile, obtained from the surface brightness profile. The entropy illustrates the thermal history of a cluster, which is solely affected by heat gains and losses (Cavagnolo et al. 2009; Panagoulia et al. 2014), and the cooling time represents the amount of time required for the ICM to radiate all the excess heat. It is calculated using $t_{cool} = \frac{kT}{n_e(r)\Lambda(T)}$ where $\Lambda(T)$ is the cooling function (Sutherland & Dopita 1993).

The right panel of Fig. 3 shows the cooling time profile of the cluster. The central cooling time at 10 kpc is 98^{+7}_{-32} Myr, which is classified as a strong cool core (Hudson et al. 2010). The three-dimensional entropy profiles for this cluster, the Phoenix cluster, and hundreds of clusters from the ACCEPT survey (Cavagnolo et al. 2009) are shown in Fig. 4. Both CHIPS1911+4455 and the Phoenix cluster have entropy profiles that are among the coolest core clusters known. The core entropy (at 10 kpc) for CHIPS1911+4455 is $17^{+2}_{-9}\,\mathrm{keVcm}^2$, which is in the lower 5 percent of all clusters in the ACCEPT survey.

4.2. *CHIPS1911+4455: A Major Merger*

There are various ways to define morphology with X-ray data. The two particular quantities we consider are the sharpness of the peak in the surface brightness profile (peakiness) and the distance between the center of symmetry on small and large scale (symmetry), identical to what was presented in Mantz et al. (2015). The peakiness measure is a proxy for the presence of a cool core, which are typically found in relaxed clusters. On the other hand, a cluster with high symmetry implies that a cluster appears similar on small and large scales, which is also evidence that the cluster is dynamically relaxed. Given that both of these proxies probe the dynamical state of the cluster, albeit in different ways, it is unsurprising that they are correlated Mantz et al. (2015). The green points in Fig. 5 show the population of relaxed clusters in this morphology plane. For CHIPS1911+4455, the peakiness is measured to be -0.501, which is in the 96^{th} percentile of all clusters in Mantz et al. (2015)'s sample, meaning that it has a bright core and likely be a relaxed cluster. Yet, the symmetry is estimated to be 0.425, which is in the 93^{rd} percentile for disturbed clusters. The fact that CHIPS1911+4455 is simultaneously one of the strongest cool cores *and* most asymmetric clusters known is highly unusual.

4.3. *CHIPS1911+4455: A Starburst BCG*

In the two right panels of Fig. 1, we compare optical images from *Hubble* with the X-ray contours from *Chandra*. The *Hubble* images show that the red emission from the old stellar populations are relatively smooth and symmetric, while the blue emission from the young stellar populations and cool gas are clumpy, asymmetric, and extended on >30 kpc scales. Since the direction of the extended blue emission is not in the direction of any nearby galaxy, it is possible that the young stars are forming directly from the cooling ICM. The filamentary complex structures in the blue emission are similar to the emission nebula in the Phoenix cluster (McDonald et al. 2019) and other nearby cool core clusters (e.g., McDonald et al. 2011; Tremblay et al. 2015).

From the 1D optical spectra in Fig. 2, we identify several emission lines in this galaxy, including H-Balmer

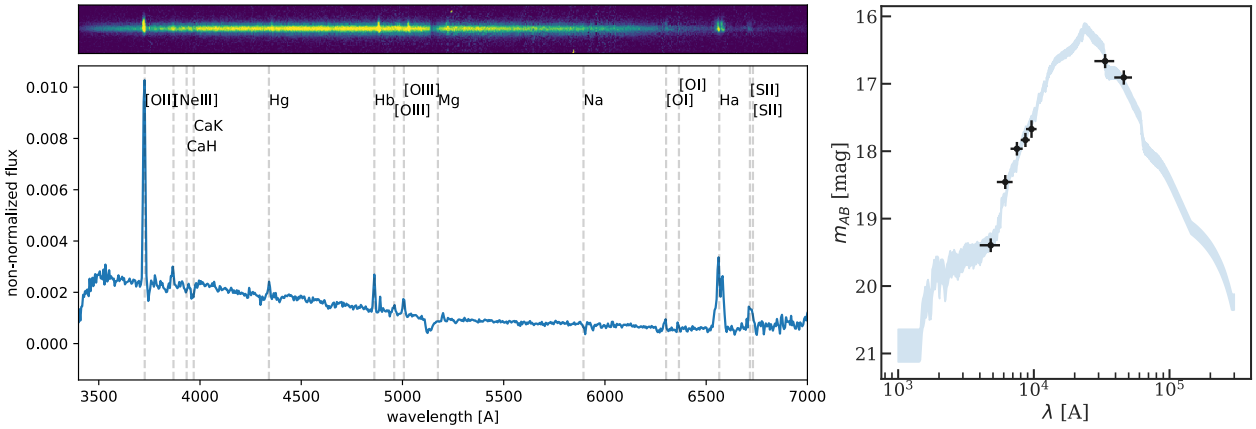

FIG. 2.— Top left: The 2D spectral image of the BCG of CHIPS1911+4455 from the Nordic Optical Telescope. Bottom left: The 1D spectrum in the rest frame from the 2D spectral image above. Grey dash lines show the location of each spectral element. The spectrum clearly shows the strong [OII] doublets at 3727 Å and the H_α emission line at 6562.8 Å. Right: The fitted spectral energy distribution (SED) model with broad-band optical data (g, r, i, z, and y) from Pan-STARRS and mid-IR from WISE.

s

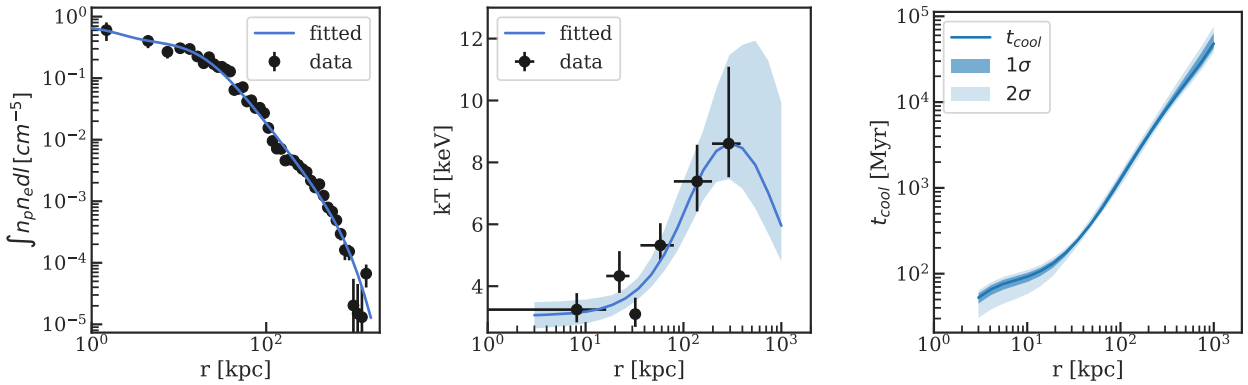

FIG. 3.— Left: The surface brightness profile of CHIPS19114455. The black dots are data points, and the blue line is the best-fit model. Middle: the projected 2-D temperature profile of the cluster. The black dots are data points extracted from the X-ray image and fit with the APEC emission model. The blue line is the best-fit model using Vikhlinin et al. (2006)'s model. Right: The cooling time profile of the cluster. The cyan-shaded region corresponds to 1σ credible region from the bootstrap while the light blue-shaded region corresponds to 2σ credible region. With the central cooling time is less than 1 Gyr, the cluster is classified as a strong cool core (Hudson et al. 2010).

series, Ne, S, O with [O II] doublets as the brightest lines. The relative lack of bright [O III] lines compared to the [O II] doublet indicates that the central galaxy in CHIPS1911+4455 is a massive starburst and not a bright AGN. We also measure the redshift of the central galaxy from these emission lines to be 0.485.

With these identified emission lines, we measure the equivalent width, which is the width such that the area of a rectangle is equal to the area in a spectral line. From the two spectra, we measure the equivalent width for [O II] (3727,3729) to be 40.9 ± 1.0 Å and 41.2 ± 1.0 Å, which is consistent with each other. To convert the equivalent width to flux for the [O II] lines, the integrated spectral energy distribution (SED) of the galaxy is fit from five broad-band optical magnitudes from Pan-STARRS (g, i, r, z, and y) (Tonry et al. 2012) and two broad-band mid-IR from WISE ($w1$ and $w2$) (Wright et al. 2010). We modeled the SED with a linear combination of "young" and "old" stellar population, and the dust reddening from starburst galaxies (Calzetti et al. 2000). The fitted SED model is shown in the right panel of Fig. 2. From the SED fit, the continuum flux at the location of [OII] (3727,3729) doublet is $9 \pm 1 \times 10^{-15}$ erg s^{-1} cm^{-2}, implying that the SFR of the central galaxy is 120^{+14}_{-15} M$_\odot$ yr^{-1} from Kennicutt (1998).

Another way to measure SFR is to use the 24 μm emission since mid-IR fluxes are unaffected by dust extinction, unlike UV and optical tracers. Instead, mid-IR emission comes from the reprocessed light by dust, produced from recently formed stars. Based on the WISE4 flux ($\sim 8 \times 10^{-13}$ erg s^{-1} cm^{-2}), we estimate the SFR for the central galaxy to be 143^{+31}_{-26}, M$_\odot$ yr^{-1}, using the SFR calibration from Cluver et al. (2017).

With both methods, we obtain consistent SFRs of $\sim$120–140 M$_\odot$ yr^{-1} which is in the top five of clusters with the most massive star formation rates.

5. DISCUSSION

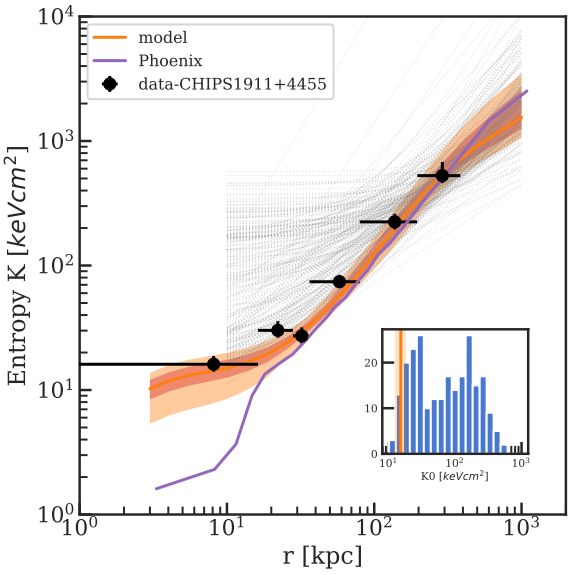

FIG. 4.— Entropy profile for CHIPS1911+4455 (orange), compared to 239 clusters from the ACCEPT survey (Cavagnolo et al. 2009) (gray) and the Phoenix cluster (purple). The shaded region corresponds to 1σ and 2σ credible region from the bootstrap. The black dots are data points, estimated from the projected 2D temperature data and the 3D density fitted model. The inset shows the histogram of the core entropy (10 kpc) of all the ACCEPT clusters and CHIPS1911+4455 (orange). CHIPS1911+4455's core entropy is at the 3.5th percentile of all ACCEPT clusters' cores entropy.

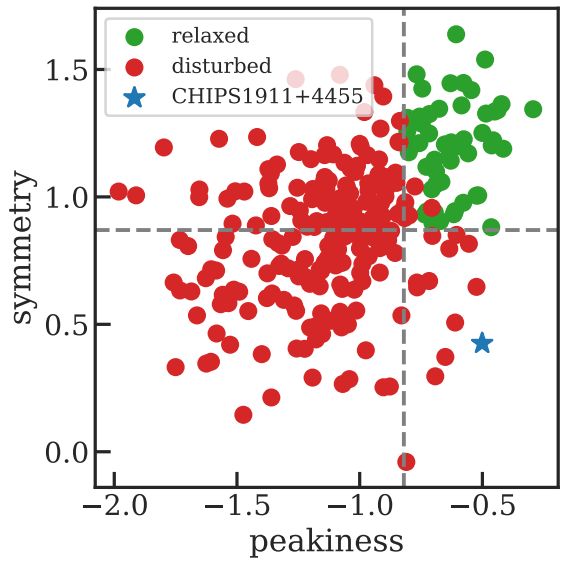

FIG. 5.— Distribution of measured morphological values for clusters from (Mantz et al. 2015). Dash lines define the relaxes samples, which are shown in green points while red points show disturbed clusters. The blue star shows the morphology for CHIPS1911+4455. This plot demonstrates that CHIPS191+445 is a unique system.

Based on Section 4.2 and 4.3, CHIPS1911+445 is a unique system in the nearby universe ($z < 0.5$) with a large star formation in the BCG even though its large-scale morphology is more similar to a disturbed cluster. It is common knowledge that at low-redshift, the most star-forming BCGs tend to be located in the most relaxed, cool-core clusters (Cavagnolo et al. 2008; Donahue et al. 2010) (e.g., Abell 1835 and the Phoenix cluster). Whereas, the star formation rate in high-redshift BCGs tend to be higher in dynamically active, non cool-core clusters (McDonald et al. 2016; Bonaventura et al. 2017). This implies that CHIPS1911+4455 is the first nearby counterpart of a high starburst-hosting BCG inside an ongoing/recent merger. Further studies of CHIPS1911+4455 may allow us to understand more about these distant high star-formation BCGs, which are much more difficult to study with our current technologies and instruments.

In the precipitation theory for regulating star formation in galaxy clusters, stars are formed when $t_{\rm cool}/t_{\rm ff} < 10$ where $t_{\rm cool}$ is the cooling time for the local gas and $t_{\rm ff}$ is the free fall time (Voit et al. 2015). There are two ways to cross this threshold which is either decreasing $t_{\rm cool}$ or increasing $t_{\rm ff}$. In the first scenario, the gas starts to cool from radiation which reduces its temperature and lessens $t_{\rm cool}$. However, an AGN accretes cooler gas, leading to AGN feedback, preventing the gas from cooling and stopping star formation. In the second scenario, the dense cool core is physically displaced from the center of a gravitational potential well, increasing $t_{\rm ff}$ at the new location. This means the gas can now cool faster than the free fall time, and eventually form stars. This scenario does not trigger AGN feedback, unlike when we decrease $t_{\rm cool}$. One possible mechanism to displace a cool core from the center is an interaction with other clusters via a major merger. The latter scenario may explain what has happened to CHIPS1911+4455: the high star formation rate is a result of a low-entropy gas being displaced from the central AGN by bulk motions induced by a major merger. This system provides evidence that cluster mergers can, in fact, stimulate star formation and enhance cooling, especially in the distant universe when mergers were more common compared to present time (Fakhouri et al. 2010).

Looking closely at the X-ray *Chandra* image in Fig 1, we see a disturbed cool core or even two distinct cool cores. When we match the locations of the two possible cool cores with the *Hubble* images, only the southern one has a galaxy counterpart while the northern one does not correspond to any particular galaxy. This suggests that the second cool core might be dense gas that is dislodged from the first cool core which remains at the location of the BCG. In addition, the blue complex filaments in the *Hubble* images are extended in the same direction toward the second cool core. In fact, the second cool core coincides with a blue clump in the northern direction of the optical images, suggesting that the shifted dense gas cools at the new location as it falls back toward the center. We also predict the direction of a merger to be along the line of the two cool cores.

6. CONCLUSION

In this work, we present new data from *Hubble*, *Chandra*, and the Nordic Optical Telescope. These data give

us more detailed looks of CHIPS1911+4455 both in the central BCG and as a whole. In particular, the optical spectra allow us to measure star formation of its BCG and link it to the morphology of the cluster in X-ray while the high-resolution optical images tell us more about the environment near the BCG. Our finding are summarized as follows:

1. From high-resolution *Chandra* X-ray image, we measure the core density of CHIPS1911+4455 at 10 kpc to be 0.0884 cm^{-3}, which is typical for a cool-core cluster. The core entropy is 17^{+2}_{-9} keVcm^2, which is within the lowest five percent of all core entropy profiles from the ACCEPT samples (Cavagnolo et al. 2009). The low core entropy is a clear signature for a massive cooling flow in the center of the cluster.

2. The X-ray morphology from an adaptively smooth X-ray image shows a peaky cluster (in the 96$^{\rm th}$ percentile of all clusters in Mantz et al. (2015)) similar to many relaxed cool-core clusters, but highly asymmetric (in the 93$^{\rm rd}$ percentile) which is comparable to a dynamically active cluster. This contradiction in its morphology between a relaxed cluster and a disturbed one is what makes this system unique and in need of further investigation.

3. The *Hubble* images show complex blue filaments near the BCG, which is an indication for a cooling flow. In addition, the images only show one giant elliptical galaxy in the center of cluster. This implies that the observed cooling is not triggered by a galaxy merging with the BCG, but instead by the cooling flow from the hot ICM.

4. With the [OII] emission doublets from NOT optical spectra, we measure SFR of the BCG to be $120^{+14}_{-15}\,M_\odot\,yr^{-1}$. We also estimate SFR using the mid-IR (via the WISE4 band) to be $143^{+31}_{-26}\,M_\odot\,yr^{-1}$. The two measured SFRs are consistent with each other and considered to be in the top five of all clusters with massive star formation rates.

5. One possible scenario for the system is a strong cool-core cluster is passed through by a smaller cluster. Parts of the cool core from the more massive cluster is dragged away from the center. As the dense gas is leaving the core and later falling back to the central potential, it cools and forms a cooling flow with a large starburst. This suggests that cluster mergers can be another avenue for clusters to enhance cooling, instead of suppressing it.

CHIPS1911+4455 is the first low-redshift ($z < 1$) galaxy cluster with this new characteristic (hosting a high star-forming BCG and a strong cool-core but having a disturbed morphology). The cluster was discovered by the Clusters Hiding in Plain Sight (*CHiPS*) survey because of its exceptionally bright cool core that appears to be point-like in previous X-ray cluster catalogs (Somboonpanyakul et al. 2018). CHIPS1911+4455 represents a unique opportunity to understand the relationship between a merging galaxy cluster and star formation in its BCG, which, in turn, unravels an alternative method to form cooling flows and massive starbursts apart from a simple accretion model. This mechanism will become much more important at high redshift ($z > 1$) when the cluster merger rate is significantly higher (Fakhouri et al. 2010; McDonald et al. 2016).

Acknowledgments.
Facilities: Pan-STARRS, *Chandra* X-ray Observatory (ACIS), *Hubble* Space Telescope (ACS/WFC), the Nordic Optical Telescope (ALFOSC)
Software: astropy (Astropy Collaboration et al. 2018), CIAO (Fruscione et al. 2006), seaborn (Waskom et al. 2016)
T. S. and M. M. acknowledge support from the Kavli Research Investment Fund at MIT, and from NASA through Chandra grant GO5-16143. The data presented here were obtained in part with ALFOSC, which is provided by the Instituto de Astrofisica de Andalucia (IAA) under a joint agreement with the University of Copenhagen and NOTSA.

REFERENCES

Abolfathi, B., Aguado, D. S., Aguilar, G., et al. 2018, ApJS, 235, 42
Astropy Collaboration, Price-Whelan, A. M., Sipőcz, B. M., et al. 2018, AJ, 156, 123
Bîrzan, L., McNamara, B. R., Nulsen, P. E. J., et al. 2008, ApJ, 686, 859
Bonaventura, N. R., Webb, T. M. A., Muzzin, A., et al. 2017, MNRAS, 469, 1259
Burns, J. O., Loken, C., Gomez, P., et al. 1997, Galactic Cluster Cooling Flows, 21
Burns, J. O., Hallman, E. J., Gantner, B., et al. 2008, ApJ, 675, 1125
Calzetti, D., Armus, L., Bohlin, R. C., et al. 2000, ApJ, 533, 682
Cavagnolo, K. W., Donahue, M., Voit, G. M., et al. 2008, ApJ, 683, L107
Cavagnolo, K. W., Donahue, M., Voit, G. M., et al. 2009, ApJS, 182, 12
Chambers, K. C., Magnier, E. A., Metcalfe, N., et al. 2016, arXiv e-prints, arXiv:1612.05560
Cluver, M. E., Jarrett, T. H., Dale, D. A., et al. 2017, ApJ, 850, 68
Crawford, C. S., Allen, S. W., Ebeling, H., et al. 1999, MNRAS, 306, 857
Donahue, M., Bruch, S., Wang, E., et al. 2010, ApJ, 715, 881
Fabian, A. C. 1994, ARA&A, 32, 277
Fabian, A. C. 2012, ARA&A, 50, 455
Fakhouri, O., Ma, C.-P., & Boylan-Kolchin, M. 2010, MNRAS, 406, 2267
Fruscione, A., McDowell, J. C., Allen, G. E., et al. 2006, Proc. SPIE, 62701V
Gómez, P. L., Loken, C., Roettiger, K., et al. 2002, ApJ, 569, 122
Gunn, J. E., Siegmund, W. A., Mannery, E. J., et al. 2006, AJ, 131, 2332
Hlavacek-Larrondo, J., McDonald, M., Benson, B. A., et al. 2015, ApJ, 805, 35
Hudson, D. S., Mittal, R., Reiprich, T. H., et al. 2010, A&A, 513, A37
Kennicutt, R. C. 1998, ARA&A, 36, 189
Mantz, A. B., Allen, S. W., Morris, R. G., et al. 2015, MNRAS, 449, 199
McDonald, M., Veilleux, S., & Mushotzky, R. 2011, ApJ, 731, 33
McDonald, M., Bayliss, M., Benson, B. A., et al. 2012, Nature, 488, 349
McDonald, M., Benson, B. A., Vikhlinin, A., et al. 2013, ApJ, 774, 23
McDonald, M., Benson, B. A., Vikhlinin, A., et al. 2014, ApJ, 794, 67
McDonald, M., Stalder, B., Bayliss, M., et al. 2016, ApJ, 817, 86

McDonald, M., Allen, S., Bayliss, M., et al. 2017, ApJ, 843, 28
McDonald, M., Gaspari, M., McNamara, B. R., et al. 2018, ApJ, 858, 45
McDonald, M., McNamara, B. R., Voit, G. M., et al. 2019, ApJ, 885, 63
McNamara, B. R., Rafferty, D. A., Bîrzan, L., et al. 2006, ApJ, 648, 164
McNamara, B. R. & Nulsen, P. E. J. 2012, New Journal of Physics, 14, 055023
Menanteau, F., Hughes, J. P., Sifón, C., et al. 2012, ApJ, 748, 7
Molendi, S. & Pizzolato, F. 2001, ApJ, 560, 194
Panagoulia, E. K., Fabian, A. C., & Sanders, J. S. 2014, MNRAS, 438, 2341
Poole, G. B., Babul, A., McCarthy, I. G., et al. 2008, MNRAS, 391, 1163
Rafferty, D. A., McNamara, B. R., & Nulsen, P. E. J. 2008, ApJ, 687, 899
Russell, H. R., Fabian, A. C., Sanders, J. S., et al. 2010, MNRAS, 402, 1561
Somboonpanyakul, T., McDonald, M., Lin, H. W., et al. 2018, ApJ, 863, 122
Sun, M. 2009, ApJ, 704, 1586
Stalder, B., Stark, A. A., Amato, S. M., et al. 2014, Proc. SPIE, 91473Y
Sutherland, R. S., & Dopita, M. A. 1993, ApJS, 88, 253
Tonry, J. L., Stubbs, C. W., Lykke, K. R., et al. 2012, ApJ, 750, 99
Tremblay, G. R., O'Dea, C. P., Baum, S. A., et al. 2015, MNRAS, 451, 3768
Vikhlinin, A., Kravtsov, A., Forman, W., et al. 2006, ApJ, 640, 691
Voit, G. M., Donahue, M., Bryan, G. L., et al. 2015, Nature, 519, 203
Waskom, M., Botvinnik, O., drewokane, et al. 2016, Seaborn: V0.7.1 (June 2016), v0.7.1, Zenodo, doi:10.5281/zenodo.54844
Wright, E. L., Eisenhardt, P. R. M., Mainzer, A. K., et al. 2010, AJ, 140, 1868